Quantum centrality testing on directed graphs via PT-symmetric quantum walks

J. A. Izaac,[1,*] J. B. Wang,[1,†] P. C. Abbott,[1] and X. S. Ma[2]

[1]*School of Physics, The University of Western Australia, Perth, Western Australia 6009, Australia*
[2]*School of Physics, Collaborative Innovation Center of Advanced Microstructures, Nanjing University, Nanjing 210093, China*

Various quantum-walk-based algorithms have been proposed to analyze and rank the centrality of graph vertices. However, issues arise when working with directed graphs: the resulting non-Hermitian Hamiltonian leads to nonunitary dynamics, and the total probability of the quantum walker is no longer conserved. In this paper, we discuss a method for simulating directed graphs using PT-symmetric quantum walks, allowing probability-conserving nonunitary evolution. This method is equivalent to mapping the directed graph to an undirected, yet weighted, complete graph over the same vertex set, and can be extended to cover interdependent networks of directed graphs. Previous work has shown centrality measures based on the continuous-time quantum walk provide an eigenvectorlike quantum centrality; using the PT-symmetric framework, we extend these centrality algorithms to directed graphs with a significantly reduced Hilbert space compared to previous proposals. In certain cases, this centrality measure provides an advantage over classical algorithms used in network analysis, for example, by breaking vertex rank degeneracy. Finally, we perform a statistical analysis over ensembles of random graphs, and show strong agreement with the classical PageRank measure on directed acyclic graphs.

I. INTRODUCTION

Quantum walks, the quantum analog of the classical random walk, were first introduced by Aharonov *et al.* [1] in his seminal paper. Since then, they have become an important tool in the field of quantum computation and quantum information theory, enabling the creation of quantum algorithms faster than their classical counterparts [2–10], finding use in modeling complex quantum dynamical systems (such as photosynthesis and electron transport [11–14]), and providing a universal method of quantum computation [15,16]. This is due, in part, to the markedly differing behavior of the quantum walk; evolving as per the Schrödinger equation, the quantum walk is a time-reversible rather than a diffusive Markovian process. Coupled with inherent quantum effects such as superposition, interference, and quantum correlations, quantum walks have therefore become an integral tool in linking network analysis and modeling with the problem-solving potential of quantum computation.

One disadvantage, however, of the quantum walk is the condition of unitarity due to the quantum nature of the walkers. As such, the standard quantum walk is unable to model or analyze directed network structures, without either (a) resulting in nonunitary dynamics or (b) modifying the framework. This serves as a particular hindrance in extending established quantum algorithms (e.g., quantum search, centrality measures, graph isomorphism) and quantum dynamical models (such as transport of electrons or excitons) to systems with directions or biased potentials. Compare this to a classical random walk, where as long as the transition matrix remains stochastic, directed networks pose no problem. Consequently, various workarounds have been proposed for dealing with this nonunitary behavior, for example, Szegedy quantum walks [10,17] and open-quantum walks [17,18]. Unfortunately, there

are numerous downsides to these approaches, each requiring a significantly expanded Hilbert space, while not guaranteeing probability conservation of the system under study or muting the effect of quantum behavior (due to environmental dephasing and loss in the open-quantum walk).

An alternative solution to this issue arrives in the form of PT symmetry. First discovered by Bender and Boettcher [19], PT symmetry started off as a simple curiosity (the appearance of non-Hermitian Hamiltonians that exhibit a real eigenspectra), thus allowing nonunitary probability conservation via a redefinition of the Hilbert space inner product. This was attributed to parity-time symmetry of the non-Hermitian Hamiltonian, and over time was generalized to allow for non-Hermitian Hamiltonian symmetry under a combination of *any* linear and nonlinear operators [19–23]. Simultaneously, PT-symmetric Hamiltonians were finding use in theoretical models of observed and predicted phenomena in condensed matter [24], quantum field theory [25,26], and being observed and implemented in numerous optical experiments [27–30], while older non-Hermitian studies in condensed matter [31] and nuclear physics [32] have been reformulated in the PT-symmetry framework [33]. Recently, PT symmetry has been used to model directed one-dimensional discrete-time quantum walks (DTQWs) [34], and considered in the case of continuous-time quantum walks (CTQWs) [35].

In this work, we present a rigorous framework for PT-symmetric CTQWs, extending the formalism of Salimi and Sorouri [35] to ensure the initial quantum state vector is preserved. This is then broadened to the cases of multiparticle systems and interdependent networks. By expanding on the work of [36], in which the CTQW was shown to provide an eigenvectorlike centrality measure for the quantum realm, we are then able to utilize the PT-symmetric CTQW to measure vertex centrality in several directed graph examples. We show that our centrality scheme compares well to the classical PageRank algorithm [37] in the case of directed acyclic graphs (DAGs) and in some cases even breaks the vertex rank degeneracy characterized by the PageRank.

---
[*]josh.izaac@uwa.edu.au
[†]jingbo.wang@uwa.edu.au

Unlike previous quantum centrality measures [10,17,18], for a graph of N vertices this scheme requires a Hilbert space of dimension N (compare this to the Szegedy quantum-walk-based PageRank scheme, which requires an N^2-dimensional Hilbert space), and without the classical decoherence required for open-quantum systems. Furthermore, we show that this formalism is equivalent to considering an undirected, yet weighted, complete graph with self-loops, providing a structural interpretation that may lead to simple experimental implementation.

This paper is structured as follows. In Sec. II, we detail the standard CTQW, and briefly discuss the issues with extending this to directed graphs. A brief introduction to the PT symmetry and pseudo-Hermitian formalism is presented in Sec. III, tailored towards a quantum walker application. In Sec. IV, we introduce our framework for PT-symmetric continuous-time quantum walks, and discuss how this can be interpreted as a mapping to a weighted and undirected CTQW on a complete graph; the framework is then extended to multiparticle systems and interdependent networks. A potential application, network centrality, is presented in Sec. V, and a statistical analysis performed to verify its performance over an ensemble of randomly generated Erdős-Rényi and scale-free graphs. Finally, our conclusions are provided in Sec. VI.

II. CONTINUOUS-TIME QUANTUM WALKS

Consider an arbitrary undirected graph $G(V,E)$, composed of vertices $j \in V$ and edges $(i,j) \in E$. The adjacency matrix of G is then defined as

$$A_{ij} = \begin{cases} 1, & (i,j) \in E \\ 0, & (i,j) \notin E. \end{cases} \quad (1)$$

For a continuous-time quantum walk on graph G, the Hamiltonian is given by the discrete Laplacian (or graph Laplacian) of the adjacency matrix:

$$H_{ij} = \left(\sum_k A_{ik} \right) \delta_{ij} - A_{ij}. \quad (2)$$

To find the time evolution of the walker, we solve the Schrödinger equation, assuming for simplicity atomic units ($m_e = e = \hbar = 1$)

$$i \frac{d}{dt} |\psi(t)\rangle = H |\psi(t)\rangle, \quad (3)$$

which has the formal solution

$$|\psi(t)\rangle = e^{-iHt} |\psi(0)\rangle. \quad (4)$$

Note that the complex-valued state vector $|\psi(t)\rangle = \sum_j a_j(t) |j\rangle$, where $a_j(t) = \langle j|\psi(t)\rangle \in \mathbb{C}$ represents the probability amplitude of the walker being found at node j at time t, with $|a_j(t)|^2 = |\langle j|\psi(t)\rangle|^2$ the resulting probability. Unlike discrete-time formulations of the quantum walk, in which probability amplitudes can only transition between adjacent (or "local") vertices at each time step, the CTQW is a *global* process. That is, it is possible for probability amplitude to transition to nonadjacent vertices in the graph at each infinitesimal time step Δt.

As the adjacency matrix A is real and symmetric, it is a Hermitian matrix, and it is easy to see from Eq. (2) that H must also be Hermitian. It therefore follows that the time-evolution operator $U = e^{-iHt}$ is unitary ($UU^\dagger = I$), guaranteeing that the norm of $|\psi(t)\rangle$ is conserved under a continuous-time quantum walk, as required.

Let us now modify G so that it is a *directed* graph, that is, the edge set $(i,j) \in E$ is now described by an *ordered* pair of vertices. As the adjacency matrix is no longer symmetric ($A_{ij} \neq A_{ji} \, \forall \, i,j$), the Hamiltonian H is no longer Hermitian, and thus we no longer have unitary time evolution ($UU^\dagger \neq I$). As a consequence, the norm squared of the quantum state is no longer conserved,

$$\langle \psi(t)|\psi(t)\rangle = \langle \psi(0)|U^\dagger U|\psi(0)\rangle \neq \langle \psi(0)|\psi(0)\rangle \quad (5)$$

and may in fact grow or decay exponentially. Various modifications proposed for dealing with this nonunitary behavior (for example, Szegedy quantum walks [10,17] and open-quantum walks [17,18]) require a significantly expanded Hilbert space, resulting in considerable resource overhead in physical implementation.

III. PT SYMMETRY

While non-Hermitian Hamiltonians with complex eigenvalues result in exponentially growing or decaying time evolution, a wide variety of non-Hermitian Hamiltonians have been found to possess real eigenvalue spectra. It was first noted by Bender and Boettcher [19] that particular non-Hermitian Hamiltonians with real spectra exhibited PT symmetry, that is,

$$[H, PT] = 0, \quad (6)$$

where $\mathcal{P} : (\hat{x}, \hat{p}) \rightarrow (-\hat{x}, -\hat{p})$ is the parity transformation operator and $\mathcal{T} : (\hat{x}, \hat{p}) \rightarrow (\hat{x}, -\hat{p})$ the time reflection operator satisfying $\{\mathcal{T}, i\} = 0$ (antilinearity) [19,38]. On the basis of this observation, it was posited that invariance of a Hamiltonian under PT transformations provides a more general condition for the reality of eigenspectra than simply Hermiticity. Immediately, research into PT-symmetric Hamiltonians found it was not so clear cut; due to the antilinearity of the PT operator, a PT-invariant Hamiltonian may still undergo spontaneous symmetry breaking, leading to complex-conjugate pairs of eigenvalues [39,40]. Furthermore, although the existence of PT symmetry is a sufficient condition for real spectra, it is not necessary. This same property can be found in Hamiltonians not exhibiting PT symmetry, thus failing to account for the existence of *all* non-Hermitian Hamiltonians with real eigenspectra.

An alternative framework was put forward by Mostafazadeh [20]. Denoted pseudo-Hermiticity, it was shown that for all diagonalizable non-Hermitian Hamiltonians exhibiting a real eigenspectra, there exists a positive-semidefinite linear operator $V = \eta^\dagger \eta$ such that

$$H^\dagger = VHV^{-1}. \quad (7)$$

Additionally, it was proven that every PT-symmetric and diagonalizable Hamiltonian is pseudo-Hermitian [20]. Coupled with the fact that $V = I$ corresponds to the case of Hermitian H, it was claimed that the pseudo-Hermiticity framework is

the correct generalization of Hermiticity to non-Hermitian Hamiltonians.

Subsequent research has further explored the connections and similarities between PT symmetry and pseudo-Hermiticity [21], with a flurry of papers released proclaiming the supremacy of one or the other, in the constant struggle to be seen as the more general of the two. Of particular note, it has been shown that even though the pseudo-Hermitian similarity transform is decidedly linear, pseudo-Hermiticity is a necessary and sufficient condition for H to admit antilinear symmetry [41–43]; i.e., the condition of pseudo-Hermiticity is equivalent to the condition $[H, \Omega] = 0$, where Ω is an antilinear invertible or involutory operator. On this basis, one can conclude that any time-reversal-invariant Hamiltonian belongs to the class of pseudo-Hermitian Hamiltonians, although the converse is not true, as Ω is not always guaranteed to be $\mathcal{T}$.

These two competing frameworks were finally reconciled by Bender and Mannheim [44], who introduced the concept of *generalized PT symmetry*; here, $\mathcal{P}$ represents *any* linear operator (not just parity), and likewise $\mathcal{T}$ represents *any* antilinear operator; the chosen operators $\mathcal{P}$ and $\mathcal{T}$ need not commute. This generalized PT-symmetry condition is necessary and sufficient for reality of the characteristic equation

$$|H - \lambda I| = 0, \tag{8}$$

which results in real eigenvalues if PT and H are simultaneously diagonalizable, and complex-conjugate pairs if not.[1] Thus, a Hamiltonian with a real eigenspectra necessarily displays (generalized) PT symmetry, regardless of its diagonalizability, providing the generalization of Hermiticity so sought after in the original parity-time and pseudo-Hermiticity frameworks. From here on in, use of the term "PT symmetry" will refer to generalized PT symmetry.

Under this new, more general, framework, pseudo-Hermiticity exists as a subset of PT symmetry [22,44], and has been expanded to include cases where H is nondiagonalizable [43]; in such cases, it is no longer possible to satisfy the pseudo-Hermiticity similarity transform with a linear operator V that is positive semidefinite, leading to spontaneous symmetry breaking and complex-conjugate pairs of eigenvalues. Moreover, Bender and Mannheim [44] provide a criteria to determine whether a positive semidefinite V exists for known PT-symmetric Hamiltonians.[2] In the following section, we will briefly outline the pseudo-Hermitian operator framework, and provide a method for determining $V = \eta^\dagger \eta$ in cases where there is no spontaneous PT-symmetry breaking.

Let H be a non-Hermitian matrix. It is pseudo-Hermitian (and thus PT symmetric), if it is related by a similarity transform to a Hermitian matrix $\tilde{H}$,

$$\tilde{H} = \eta H \eta^{-1}, \tag{9}$$

where η is frequently referred to in the literature as the *pseudo-Hermitian operator* or *metric*. Without loss of generality, we assume η is an Hermitian operator ($\eta = \eta^\dagger$). Due to the properties of a similarity transform, the eigenvalues of H will be the same as $\tilde{H}$ and necessarily real. Taking the conjugate transpose of this result, we get

$$\tilde{H}^\dagger = (\eta^{-1})^\dagger H^\dagger \eta^\dagger = \eta^{-1} H^\dagger \eta. \tag{10}$$

Since $\tilde{H}$ is Hermitian, $\eta^{-1} H^\dagger \eta = \eta H \eta^{-1}$, and thus a pseudo-Hermitian matrix must satisfy the following similarity transform with its conjugate transpose:

$$H^\dagger = \eta^2 H \eta^{-2}. \tag{11}$$

Rewriting this in the form $\eta^2 H = H^\dagger \eta^2$, note that the right-hand side is simply the Hermitian conjugate of the left-hand side. This suggests that the following redefinition of the inner product,

$$\langle \ldots | \ldots \rangle_\eta := \langle \ldots | \eta^2 | \ldots \rangle, \tag{12}$$

should be sufficient to conserve the system's probability. Indeed, by using the Schrödinger equation, we see that this is in fact the case when working with pseudo-Hermitian operators:

$$\frac{d}{dt} \langle \psi(t) | \psi(t) \rangle_\eta = \left\langle \frac{d}{dt} \psi(t) \middle| \eta^2 | \psi(t) \right\rangle + \left\langle \psi(t) | \eta^2 \middle| \frac{d}{dt} \psi(t) \right\rangle$$
$$= \langle \psi(t) | i H^\dagger \eta^2 | \psi(t) \rangle - \langle \psi(t) | \eta^2 i H | \psi(t) \rangle$$
$$= i \langle \psi(t) | (H^\dagger \eta^2 - \eta^2 H) | \psi(t) \rangle$$
$$= 0.$$

As Hermitian matrices are always diagonalizable by their unitary eigenbasis ($\tilde{H} = P \Lambda P^\dagger$ where $P^{-1} = P^\dagger$), it follows from the similarity relation (9) that pseudo-Hermitian matrices must also be diagonalizable:[3]

$$H = \eta^{-1} \tilde{H} \eta = (\eta^{-1} P) \Lambda (P^\dagger \eta) = (P^\dagger \eta)^{-1} \Lambda (P^\dagger \eta).$$

Diagonalizable matrices must admit a biorthonormal eigenbasis [45]

$$H | \psi_j \rangle = \lambda_j | \psi_j \rangle, \tag{13}$$

$$H^\dagger | \phi_j \rangle = \lambda_j | \phi_j \rangle, \quad j = 1, 2, \ldots, n \tag{14}$$

where $\langle \phi_i | \psi_j \rangle = \delta_{ij}$ and $\lambda_j \in \mathbb{R}$ due to pseudo-Hermiticity. The completeness relation is given by

$$I = \sum_j | \psi_j \rangle \langle \phi_j |. \tag{15}$$

By applying the pseudo-Hermiticity relation [Eq. (11)] to the biorthonormal eigenvector equations, we can deduce a method of constructing η. For instance,

$$H^\dagger | \phi_j \rangle = \eta^2 H \eta^{-2} | \phi_j \rangle = \lambda_j | \phi_j \rangle. \tag{16}$$

---

[1]This is an example of spontaneous PT-symmetry breaking. Even though a Hamiltonian may display PT invariance (i.e., $[H, PT] = 0$), the eigenstates of H, denoted $|\phi_n\rangle$, are not necessarily simultaneously eigenstates of PT, due to the antilinearity of the PT operator. If this is the case, then the eigenspectrum is composed of complex-conjugate pairs of eigenvalues, and $PT |\phi_n\rangle$ provides the eigenstates of PT.

[2]If $[\mathcal{C}, PT] = 0 \; \forall \mathcal{C}$ such that $\mathcal{C}^2 = 1$ and $[\mathcal{C}, H] = 0$, then there exists a positive-semidefinite linear operator $V = \mathcal{C}\mathcal{P}$ such that $V H V^{-1} = H^\dagger$.

[3]In fact, solving this equation allows you to find an expression for η in terms of the left eigenvectors of H, $\langle \phi_j |$, and the eigenvectors of $\tilde{H}$, $|\tilde{\psi}_j\rangle$: $\eta_{ij} = \sum_k |\tilde{\psi}_k\rangle_i \langle \phi_j|_k$.

Premultiplying both sides by η^{-2},

$$H(\eta^{-2}|\phi_j\rangle) = \lambda_j(\eta^{-2}|\phi_j\rangle), \tag{17}$$

it can be seen that

$$|\psi_j\rangle = \eta^{-2}|\phi_j\rangle \;\Leftrightarrow\; |\phi_j\rangle = \eta^2|\psi_j\rangle. \tag{18}$$

Hence, η acts to transform between the pseudo-Hermitian and Hermitian basis, and η^2 acts to transform between the pseudo-Hermitian biorthonormal eigenbasis. It therefore follows that the biorthonormal eigenbasis is the basis for the inner product space defined by Eq. (12). Combining this result with the biorthonormal completeness relation, we arrive at a method of constructing the pseudo-Hermitian operator η:

$$\eta = \sqrt{\eta^2 \sum_j |\psi_j\rangle\langle\phi_j|} = \sqrt{\sum_j |\phi_j\rangle\langle\phi_j|} \tag{19}$$

and similarly

$$\eta^{-1} = \sqrt{\sum_j |\psi_j\rangle\langle\phi_j|\eta^{-2}} = \sqrt{\sum_j |\psi_j\rangle\langle\psi_j|}. \tag{20}$$

Since we have defined $V = \eta^2$, it follows that

$$V = \sum_j |\phi_j\rangle\langle\phi_j| \;\Leftrightarrow\; V^{-1} = \sum_j |\psi_j\rangle\langle\psi_j|. \tag{21}$$

Further, as V is positive semidefinite, we can be assured that the square-root function applied to the operators in Eqs. (19) and (20) is well defined, albeit admitting multiple solutions. For consistency, we will choose η to be the *principal square root*, the unique positive-semidefinite square root of V.

So, to briefly summarize, H is necessarily pseudo-Hermitian (and consequently PT symmetric) if it satisfies *any one* of the following equivalent conditions:

(1) *H is similar to a Hermitian matrix.* There exists a Hermitian operator η and a Hermitian matrix $\tilde{H}$ such that $\tilde{H} = \eta H \eta^{-1}$.

(2) *H is similar to its own Hermitian conjugate.* There exists a positive Hermitian operator η such that $H^\dagger = \eta^2 H \eta^{-2}$.

(3) *H has real eigenvalues and is diagonalizable.* Note that a matrix is diagonalizable if and only if it has n linearly independent eigenvectors [45].

IV. PSEUDO-HERMITIAN CONTINUOUS-TIME QUANTUM WALKS

First introduced by Salimi and Sorouri [35], pseudo-Hermitian continuous-time quantum walks take advantage of the pseudo-Hermitian structure of various graphs in order to implement directed quantum walks. In their study, the transition probability of the pseudo-Hermitian CTQW at vertex j at time t is defined to be

$$\mathbb{P}_j(t) = |\langle j|\eta e^{-iHt}|\psi(0)\rangle|^2. \tag{22}$$

Note that this does *not* preserve the initial state;

$$\mathbb{P}_j(0) = |\langle j|\eta|\psi(0)\rangle|^2 \neq |\langle j|\psi(0)\rangle|^2. \tag{23}$$

Thus, if $|\psi(0)\rangle$ is chosen to be an equal superposition over all vertices, this will not be reflected in the quantum walk at time $t = 0$, making this definition unsuitable for algorithms

such as centrality testing and graph isomorphism. Thus, rather than utilize their implementation, we present an alternative formulation.

As our aim is to experimentally produce a pseudo-Hermitian CTQW for network analysis, rather than redefine the Hilbert space inner product as per Eq. (12), the inner product will not be modified. Instead, we have three options available:

(A) *No modification*: implement the time-evolution operator using the normal framework for the CTQW, $U = e^{-iHt}$, with no redefinition of the inner product. This results in a nonunitary and non-probability-conserving time evolution, but the pseudo-Hermiticity of the system ensures the norm squared of the quantum walk wave function will just oscillate with no exponential growth and decay.

(B) *Modify the time-evolution operator*: the nonunitary time-evolution operator from (A) is instead modified as follows:

$$\tilde{U}(t) = \eta U(t)\eta^{-1} = \eta e^{-iHt}\eta^{-1}, \tag{24}$$

where $\tilde{U}(t)$ is unitary due to the pseudo-Hermitian similarity transform of the matrix exponential. This reflects the underlying directional structure of the graph, while allowing for probability conservation. Note that while the product is unitary, η and $U(t)$ are nonunitary matrices.

(C) *Modify the Hamiltonian*: in this approach, the pseudo-Hermitian Hamiltonian is modified via similarity transform to make it Hermitian,

$$\tilde{U}(t) = e^{-i\tilde{H}t} = e^{-i\eta H\eta^{-1}t}. \tag{25}$$

This preserves the directional structure of the graph, while allowing us to use the standard CTQW framework. Furthermore, it has the potential to be implemented experimentally via quantum simulation.

Note that options (B) and (C) are equivalent: it is only their resulting experimental implementations which would differ. From here on, the modified CTQW walk outlined in (B) and (C) will be referred to as the η-CTQW, to distinguish it from the standard nonunitary CTQW in (A).
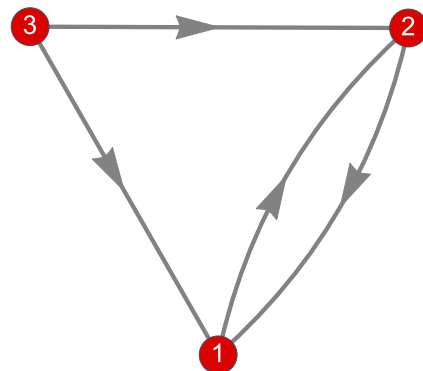

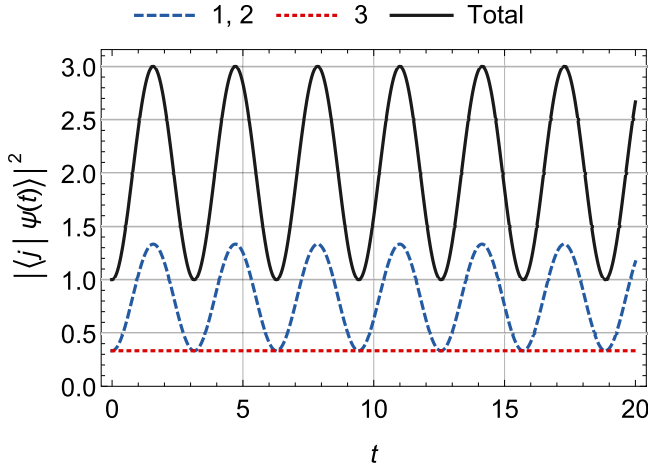FIG. 1. Three-vertex directed graph.

FIG. 2. Vertex squared norm vs time (arbitrary unit) for the nonunitary CTQW on the directed graph Fig. 1, with the walker initially in an equal superposition of vertex states $|\psi(0)\rangle = \frac{1}{\sqrt{3}} \sum_j |j\rangle$. Vertices 1 and 2 have equal norm squared (blue, dashed line), with a higher time average than vertex 3 (red, dotted line). The squared norm of the total system is given by the black, solid line.

FIG. 3. Vertex probability vs time (arbitrary unit) for the pseudo-Hermitian η-CTQW on the directed graph Fig. 1, with the walker initially in an equal superposition of vertex states $|\psi(0)\rangle = \frac{1}{\sqrt{3}} \sum_j |j\rangle$. Vertices 1 and 2 have equal probability (blue, dashed line), with a higher time average than vertex 3 (red, dotted line). The total probability of the system is given by the black, solid line.

A. Three-vertex directed graph

Consider the three-vertex graph in Fig. 1. Its Hamiltonian is found by calculating the graph Laplacian

$$H = \begin{bmatrix} 1 & -1 & -1 \\ -1 & 1 & -1 \\ 0 & 0 & 2 \end{bmatrix}. \tag{26}$$

While not Hermitian ($H^\dagger \neq H$), the eigenvalues ($\lambda = 0, 2, 2$) are all real and the eigenvectors are linearly independent; thus, H is PT symmetric and pseudo-Hermitian.

1. Standard CTQW (non-probability-conserving)

Solving the Schrödinger equation for the standard CTQW (Fig. 2), we find that although there is no exponential growth or decay of the squared norm of the wave function (due to the pseudo-Hermiticity), nevertheless, the squared norm oscillates and is not conserved.

In order to experimentally implement this CTQW, we wish to decompose the time-evolution operator such that the time dependence is restricted to a single diagonal unitary matrix. Diagonalizing H yields the following decomposition:

$$U(t) = \frac{1}{2} \begin{bmatrix} 1 & -1 & -1 \\ 1 & 0 & 1 \\ 0 & 1 & 0 \end{bmatrix} \begin{bmatrix} 1 & 0 & 0 \\ 0 & e^{-2it} & 0 \\ 0 & 0 & e^{-2it} \end{bmatrix} \begin{bmatrix} 1 & 1 & 1 \\ 0 & 0 & 2 \\ -1 & 1 & -1 \end{bmatrix}. \tag{27}$$

Note that while the diagonal matrix is unitary, the two outer matrices are nonunitary, resulting in a nonunitary time-evolution operator $U(t)$.
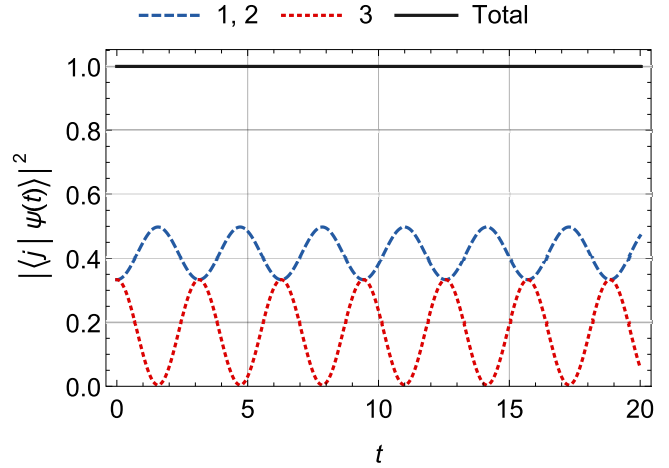
2. η-CTQW (probability conserving)

By calculating the biorthonormal eigenbasis, we can derive the pseudo-Hermitian operator η of the graph

$$\eta = \frac{1}{6} \begin{bmatrix} 3 + 2\sqrt{2} & -3 + 2\sqrt{2} & \sqrt{2} \\ -3 + 2\sqrt{2} & 3 + 2\sqrt{2} & \sqrt{2} \\ \sqrt{2} & \sqrt{2} & 5\sqrt{2} \end{bmatrix}. \tag{28}$$

Thus, the modified time-evolution operator is given by $\tilde{U}(t) = \eta e^{-iHt} \eta^{-1}$ (see Fig. 3 for how this affects the dynamics of the quantum walk).

In order to find a useful decomposition, we need to be able to diagonalize $\eta H \eta^{-1}$; i.e.,

$$D = S^\dagger \eta H \eta^{-1} S. \tag{29}$$

Once S is calculated, by similarity it can also be used to diagonalize $\tilde{U}(t)$. This results in the following decomposition:

$$\tilde{U}(t) = S \begin{bmatrix} 1 & 0 & 0 \\ 0 & e^{-2it} & 0 \\ 0 & 0 & e^{-2it} \end{bmatrix} S^\dagger, \tag{30}$$

where

$$S = \frac{1}{3} \begin{bmatrix} 2 & -\frac{3}{\sqrt{2}} & -\frac{1}{\sqrt{2}} \\ 2 & \frac{3}{\sqrt{2}} & -\frac{1}{\sqrt{2}} \\ 1 & 0 & 2\sqrt{2} \end{bmatrix}. \tag{31}$$

Note that, unlike the non-probability-conserving case, here all three of the decomposed matrices are unitary.

B. Alternative interpretation

To get an understanding of the transformation from the non-probability-conserving CTQW to the pseudo-Hermitian η-CTQW, let us have a look at the pseudo-Hermitian Hamiltonian

for the three-vertex graph discussed above:

$$\tilde{H} = \eta H \eta^{-1} = \frac{1}{9} \begin{bmatrix} 10 & -8 & -4 \\ -8 & 10 & -4 \\ -4 & -4 & 16 \end{bmatrix}. \tag{32}$$

Describing a discrete graph structure, the η-Hamiltonian $\tilde{H}$ is symmetric, yet contains fractional quantities: we may interpret $\tilde{H}$ as the Laplacian of a weighted, undirected complete graph with self-loops. (Note that this is just one valid interpretation, and is not unique.) In doing so, it is convenient to use a more rigorous definition of the Laplacian more suited to weighted graphs.

The *oriented incidence matrix M* of an undirected graph $G(V,E)$, with vertex set $V = \{v_1, v_2, \ldots, v_N\}$ and edge set $E = \{e_1, e_2, \ldots, e_m\}$, is a $n \times m$ matrix associated with a particular orientation of the edges of G. That is, each edge e_j is given a random direction. The oriented incidence matrix is therefore defined as follows:

$$M_{ij} = \begin{cases} 2, & \text{if edge } e_j \text{ is a self-loop incident on node } v_i \\ 1, & \text{if edge } e_j \text{ is incident away from node } v_i \\ -1, & \text{if edge } e_j \text{ is incident towards node } v_i \\ 0, & \text{if edge } e_j \text{ is not incident on node } v_i. \end{cases} \tag{33}$$

Note that, unlike the standard incidence matrix, columns of the oriented incidence matrix not associated with self-loops must sum to zero.

Once we have calculated the oriented incidence matrix of a weighted graph, we can compute the $N \times N$ *weighted Laplacian* using the following relationship:

$$L = MWM^T, \tag{34}$$

where W is a diagonal matrix containing the weights $\{w_{ij}\}$ associated with the edges $\{(v_i, v_j)\}$. For a complete graph over N vertices with self-loops and arbitrary edge weighting, it turns out we can compute the weighted Laplacian directly,

$$L_{ij} = \begin{cases} \sum_{k=1}^{N} w_{ik} + 3w_{ii}, & i = j \\ -w_{ij}, & i \neq j \end{cases} \tag{35}$$

where $w_{ij} = w_{ji}$ and the size of the set $\{w_{ij}\}$ is $|E| = \frac{1}{2}N(N+1)$. Thus, if we have an $N \times N$ pseudo-Hamiltonian $\tilde{H}$, then solving $\tilde{H} = L_{ij}$ provides the edge weighting

$$w_{ij} = \begin{cases} \frac{1}{4}\sum_{k=1}^{N} \tilde{H}_{ik}, & i = j \\ -\tilde{H}_{ij}, & i \neq j. \end{cases} \tag{36}$$

That is, we can interpret the η-CTQW of a *directed N*-vertex graph in terms of a standard CTQW on a *undirected* complete graph with self-loops, and edge weights given by w_{ij} above. The undirected edge weightings allows us to approximate the directed dynamics we require.

For example, let us return to the three-vertex graph examined previously. Using the pseudo-Hamiltonian of the graph [Eq. (32)], we can find the edge weights w_{ij} via Eq. (36). See Fig. 4 for the result.

C. Multiparticle η-CTQW

If we wish to extend the standard CTQW to simulate P distinguishable particles on graph G, the Hamiltonian of the
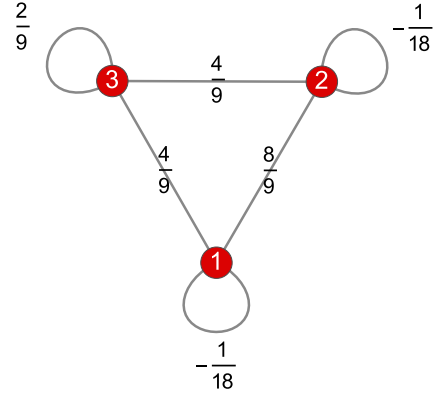

FIG. 4. Performing an η-CTQW on the three-vertex directed graph in Fig. 1 is equivalent to performing a standard CTQW on the undirected edge-weighted graph shown above.

system is expanded to act on a N^P Hilbert space, as follows:

$$H^{(P)} = H_1 \oplus H_2 \oplus \cdots \oplus H_P + \Gamma_{\text{int}}, \tag{37}$$

where H_j is the free-particle Hamiltonian of the jth particle on graph G, Γ_{int} represents a potential interaction between the particles, and $\oplus$ is the tensor or Kronecker sum defined by

$$A_{n \times n} \oplus B_{m \times m} = A_{n \times n} \otimes I_{m \times m} + I_{n \times n} \otimes B_{m \times m}. \tag{38}$$

Note that the free-particle Hamiltonians are identical ($H_1 = H_2 = \cdots = H_P$), allowing this to be rewritten as

$$H^{(P)} = H^{\oplus p} + \Gamma_{\text{int}}. \tag{39}$$

In the case of no interaction ($\Gamma_{\text{int}} = 0$), then it is trivial to show that if H is pseudo-Hermitian, then so is $H^{(P)}$, with pseudo-Hermitian operator $\eta^{(P)}$ given by

$$\eta^{(P)} = \underbrace{\eta \otimes \eta \otimes \cdots \otimes \eta}_{P} = \eta^{\otimes P}, \tag{40}$$

and η the pseudo-Hermitian operator of the single-particle Hamiltonian H.

When $\Gamma_{\text{int}} \neq 0$, then additional care must be taken; unlike Hermitian matrices, the pseudo-Hermitian matrices are *not* closed under addition, so $H^{(P)}$ is no longer guaranteed to be pseudo-Hermitian (this can easily be shown by counterexample).

D. Interdependent networks

Aside from the Cartesian product of graphs discussed above, another method of combining graph structures are interdependent networks. In the real world, very few networks operate independently, instead interacting and depending on a myriad of other networks [46,47]: examples include modeling cascading failures between power grids, communication networks, and physiological and biochemical systems. As such, being able to extend the pseudo-Hermitian CTQW to model interdependent networks greatly expands the scope of the framework. In this section, we will consider an interconnected network of two pseudo-Hermitian graphs and determine the properties that must be satisfied for the resulting network to have guaranteed pseudo-Hermiticity.

Let A_1 and A_2 refer to the adjacency matrices of two graphs G_1 and G_2, respectively. The resulting interdependent network Hamiltonian is constructed as follows:

$$A = \begin{bmatrix} A_1 & B_0 \\ B_0^T & A_2 \end{bmatrix}, \tag{41}$$

where B_0 is the adjacency matrix representing the edges connecting the two sets of vertices $V(A_1)$ and $V(A_2)$. The Hamiltonian of this graph, defined by Eq. (2), can then be written as

$$H = \begin{bmatrix} \mathcal{H}_1 & -B_0 \\ -B_0^T & \mathcal{H}_2 \end{bmatrix}, \tag{42}$$

where

$$(\mathcal{H}_u)_{ij} = (H_u)_{ij} + \sum_k (B_0)_{ik}\delta_{ij}, \ u \in \{1,2\} \tag{43}$$

and H_1 and H_2 are the Hamiltonians of A_1 and A_2, respectively.

Theorem 1. The Hamiltonian of an interdependent network of two graphs A_1 and A_2, with pseudo-Hermitian Hamiltonians H_1 and H_2, respectively, will itself exhibit pseudo-Hermiticity if the internetwork connections B_0 are pseudo-Hermitian and degree regular, and the commutation relations $H_1 B_0 = B_0 H_2$ and $H_2 B_0^T = B_0^T H_1$ are satisfied.

Proof. B_0 is degree regular with degree c; thus,

$$\sum_k (B_0)_{ik}\delta_{ij} = c\delta_{ij} \ \Rightarrow \ \mathcal{H}_u = H_u + cI. \tag{44}$$

If we decompose the Hamilton into the sum

$$H = \begin{bmatrix} \mathcal{H}_1 & 0 \\ 0 & \mathcal{H}_2 \end{bmatrix} + \begin{bmatrix} 0 & -B_0 \\ -B_0^T & 0 \end{bmatrix} = A + B, \tag{45}$$

we can now prove that the interdependent network Hamiltonian is always pseudo-Hermitian if the two components A and B commute and are themselves pseudo-Hermitian.

Since H_1 and H_2 are pseudo-Hermitian, they are therefore diagonalizable by matrices Q_u:

$$\Lambda_u = Q_u^{-1} H_u Q_u, \tag{46}$$

where Λ_u are real diagonal matrices of eigenvalues. It follows that

$$Q_u^{-1}\mathcal{H}_u Q_u = Q_u^{-1}(H_u + cI)Q_u = \Lambda_u + cI. \tag{47}$$

That is, $\mathcal{H}_1$ and $\mathcal{H}_2$ are simultaneously diagonalizable and exhibit real eigenspectra, satisfying the criteria for pseudo-Hermiticity. From here, it is trivial to show that A is diagonalized as follows:

$$\Lambda_A = \begin{bmatrix} \Lambda_1 + cI & 0 \\ 0 & \Lambda_2 + cI \end{bmatrix} = Q_A^{-1} A Q_A, \tag{48}$$

where

$$Q_A = \begin{bmatrix} Q_1 & 0 \\ 0 & Q_2 \end{bmatrix} \tag{49}$$

and Λ_A is real.

As B_0 is also pseudo-Hermitian, therefore, it is also diagonalizable with real eigenvalues: $\Lambda_{B_0} = Q_{B_0}^{-1} B_0 Q_{B_0}$. Similarly to above, we can use this result to diagonalize the matrix B:

$$\Lambda_B = \begin{bmatrix} \Lambda_{B_0} & 0 \\ 0 & -\Lambda_{B_0} \end{bmatrix} = Q_B^T B Q_B, \tag{50}$$
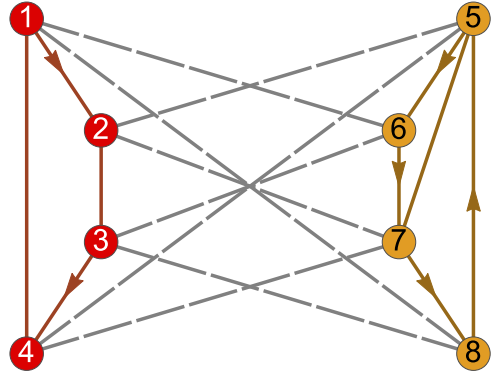

FIG. 5. A pseudo-Hermitian interconnected network composed of two four-vertex pseudo-Hermitian graphs (red and yellow, respectively) connected via circulant interconnections (gray, dashed line).

where

$$Q_B = \frac{1}{\sqrt{2}}\begin{bmatrix} Q_{B_0} & Q_{B_0} \\ Q_{B_0} & -Q_{B_0} \end{bmatrix} \tag{51}$$

and Λ_B is real.

It follows from the above analysis that if H_1 and H_2 are pseudo-Hermitian, and the interconnections adjacency matrix B_0 is pseudo-Hermitian and degree regular, that the matrices A and B are also pseudo-Hermitian.

To ensure that the sum $A + B$ remains pseudo-Hermitian, we can make use of the well-known property that commutating diagonalizable matrices are simultaneously diagonalizable [48]. This requires the additional constraint $[A, B] = 0$, resulting in the following two conditions that must be satisfied:

$$H_1 B_0 = B_0 H_2, \tag{52a}$$
$$H_2 B_0^T = B_0^T H_1. \tag{52b}$$

If these are both satisfied, then A and B must be simultaneously diagonalized by a matrix S:

$$H = A + B = S\big(P_A \Lambda_A P_A^T + P_B \Lambda_B P_B^T\big)S^{-1}, \tag{53}$$

where P_A and P_B are permutation matrices. From here, we can see that the eigenvalues of H are contained in the set of elements $\{\lambda_1 \pm \lambda_{B_0} + 1\} \cup \{\lambda_2 \pm \lambda_{B_0} + 1\}$ and thus are necessarily real. Therefore, the interdependent network of pseudo-Hermitian graphs, which commute with their interconnections, also exhibits pseudo-Hermiticity. ∎

An example of a pseudo-Hermitian interconnected network in which the two graph Hamiltonians commute with the interconnections is given in Fig. 5. Note that the above theorem is not a necessary condition for interdependent network pseudo-Hermiticity: examples can be constructed where $[A, B] \neq 0$, yet $A + B$ remains diagonalizable and pseudo-Hermitian. Nevertheless, this result provides a useful method of constructing interdependent networks with guaranteed pseudo-Hermiticity.

V. CENTRALITY TESTING

A. Centrality introduction

In the study of network structure, centrality measures are an integral tool, allowing the determination and ranking of graph nodes deemed more important to the structure [37,49–54]. At its core, a graph centrality measure satisfies the following properties:

(i) $C : G(V,E) \rightarrow \mathbb{R}^{|V|}$ is a function or algorithm that accepts a graph as input, and returns a real valued, strictly positive vector over the set of vertices V.

(ii) The highest values obtained correspond to vertices deemed more "important" or "central" to the graph structure.

However, with this general definition comes several caveats. First, note that no meaning has been attributed to vertices with low centrality values; this is deliberate, as noise grows successively larger for vertices beyond the topmost ranked vertices [55]. As such, centrality measures convey very little information regarding a majority of vertices; they are solely for determining the most central nodes (ranking *all* the vertices is more the domain of *influence measures* [56]). Second, what constitutes "importance" is subjective, and depends on the application or model to be analyzed, and how information "flows" throughout the network [57].

To account for the numerous ways we may quantify importance, various methods exist for measuring how central or important particular vertices are in a network structure; degree centrality, closeness centrality, eigenvector centrality, PageRank centrality, to name a few. It is pertinent to note that many of these centrality measures can be reformulated as classical random walks. For instance, the degree centrality is based on walks of length one, and is useful in models requiring direct and immediate influence between adjacent nodes. Moreover, it is trivial to show that the degree centrality is proportional to the limiting distribution of a random walk [58].

Eigenvector centrality, on the other hand, is a useful measure when considering long-term "indirect" influence between vertices; if a vertex with low degree is adjacent to a vertex with a high number of connections, the first vertex will likewise have a high eigenvector centrality measure [57]. Based on the spectral properties of a graph, the eigenvector centrality is defined by $C_j^{(ev)} = \mathbf{v}_j$, where $\mathbf{v}$ is the eigenvector of the adjacency matrix with maximum eigenvalue [59]. Also referred to as the *principal eigenvector*, it is chosen to ensure (via the Perron-Frobenius theorem, assuming that A is irreducible) that the ranking $C_j^{(ev)}$ remains strictly positive. It has been shown by Bonacich [60] that

$$\mathbf{v}_j \propto \sum_i \sum_{n=1}^{\infty} \lambda^{1-n}(A^n)_{ij}, \tag{54}$$

where λ is the maximum (principal) eigenvalue. As $(A^n)_{ij}$ represents the number of walks of length n between vertices i and j, it can be seen that the eigenvector centrality performs walks of *all* lengths, weighted inversely by length, from each node. It should be noted that this result allows us to draw interesting parallels with the CTQW; consider the CTQW time-evolution operator for infinitesimal time dt:

$$U(t) = e^{-iHdt} = \sum_{n=0}^{\infty} \frac{1}{n!}(-idt)^n H^n. \tag{55}$$

That is, like the eigenvector centrality, the CTQW performs walks of all lengths at each infinitesimal time step dt, weighted inversely by walk length. Thus, at the very least, the CTQW may provide the means for an eigenvectorlike quantum centrality measure.

Unfortunately, the classical eigenvector centrality can provide ineffectual results when applied to directed graphs, for a multitude of reasons. For example, vertices not in a strongly connected component will be assigned an eigenvector vertex centrality of 0, as A is no longer irreducible and the Perron-Frobenius theorem is no longer valid. Furthermore, "dangling nodes" (vertices or components with in-degree and zero out-degree) found in directed acyclic subgraphs can result in the eigenvector centrality "localizing" or accumulating at the affected vertices [61,62]. Furthermore, in the case of directed acyclic graphs, the eigenvector centrality provides no useful centrality information whatsoever: the centrality measure of every vertex is identically assigned to be zero.

To rectify these issues, a wide range of variations to the eigenvector centrality have been proposed, including PageRank and Katz centrality. Of these, PageRank is arguably the most well known spectral centrality measure, due to its use in the Google search engine [37]. Designed to take into account directed networks, the PageRank improves on the eigenvector centrality by modifying the adjacency matrix to ensure stochasticity and irreducibility, while also introducing a "random surfer effect," a nonzero probability $1 - \alpha$ (where $\alpha \in [0,1]$) that a walker at a vertex can transition to *any* other adjacent or nonadjacent vertex. In practice, α is generally chosen to be 0.85, providing a good compromise between information flow via hyperlinks and the random surfer effect. Note that, while a modification of the eigenvector centrality, the PageRank's use of a stochastic transition matrix consequently allows it to be modeled in terms of a random walk of length one at each time step.

Due to the close relationship between centrality measures and classical measures, directed quantum walks provide a natural starting point for exploring quantum centrality algorithms. For example, the quantum PageRank algorithm utilizes the discrete-time Szegedy quantum walk [10,17], while the quantum stochastic walk (QSW) makes use of its hybrid classical-quantum regime to rank centrality of directed graphs [17,18]. However, both approaches have their drawbacks; both require expanding the Hilbert space beyond that required for a standard quantum walk, hindering practical implementation, with additional classical decoherence suppressing quantum behavior in the QSW. The CTQW also naturally lends itself to centrality analysis, and may provide a quantum analog to the eigenvector centrality, minus issues due to nonstochasticity and nonirreducibility due to its quantum propagation. Unfortunately, as the CTQW is not defined for directed and non-Hermitian graphs, possible applications regarding spectral centrality analysis has not been fully explored in the literature. Fortuitously, the pseudo-Hermitian η-CTQW extends the CTQW formalism to directed graphs, while preserving the eigenspectrum of the original graph.

In this section, we propose a quantum centrality measure based on the pseudo-Hermitian η-CTQW, which has the advantage of a purely quantum propagation and smaller state space than both the quantum PageRank and QSW.

B. Proposed quantum scheme and examples

Taking a similar approach to the quantum PageRank, we propose the following measure for assigning a centrality value to vertex j on a directed graph represented by the pseudo-Hermitian Hamiltonian H:

$$v_j = \lim_{T \to \infty} \frac{1}{T} \int_0^T \left| \langle j | e^{-i\eta H \eta^{-1} t} \left(\frac{1}{\sqrt{N}} \sum_k |k\rangle \right) \right|^2 dt. \quad (56)$$

Note that this method simply requires a Hilbert space of dimension N. This scheme will then be applied to the three-vertex graph discussed previously.

First, consider the non-probability-conserving standard CTQW walk in the previous section. As the pseudo-Hermitian Hamiltonian preserves the graph eigenspectra, we expect the resulting dynamics to reflect properties that can be classically extracted from the spectra, such as vertex centrality. Thus, one potential way of extracting this information is simply to calculate the time average of the probability on each vertex, and normalize it by the total probability time average.

Solving the Schrödinger equation for the unmodified Hamiltonian evolving the initial state $|\psi(0)\rangle = \frac{1}{\sqrt{3}}(|1\rangle + |2\rangle + |3\rangle)$, we get the exact solution

$$|\psi(t)\rangle = \frac{1}{\sqrt{6}}\sqrt{5 - 3\cos(2t)}(|1\rangle + |2\rangle) + \frac{1}{\sqrt{3}}|3\rangle, \quad (57)$$

where

$$\langle \psi(t)|\psi(t)\rangle = 2 - \cos(2t). \quad (58)$$

The total probability has a time average over $t = [0, \pi]$ (one period) of

$$\int_0^\pi \langle \psi(t)|\psi(t)\rangle \, dt = 2\pi, \quad (59)$$

therefore, calculating the time average of this result over $t = [0, \pi]$:

$$\frac{1}{2\pi} \int_0^\pi |\langle j|\psi(t)\rangle|^2 dt = \frac{5}{12}\langle j|1\rangle + \frac{5}{12}\langle j|2\rangle + \frac{1}{6}\langle j|3\rangle. \quad (60)$$

That is, by this centrality measure, vertices 1 and 2 are ranked equal first, followed by vertex 3.

Next, consider the probability-conserving η-CTQW case $\tilde{U}(t) = \eta e^{-iHt}\eta^{-1}$. As we have an exact representation of η, we are also able to solve for $|\tilde{\psi}(t)\rangle$ exactly:

$$|\tilde{\psi}(t)\rangle = \frac{1}{\sqrt{243}}\sqrt{101 - 20\cos(2t)}(|1\rangle + |2\rangle)$$

$$+ \frac{1}{\sqrt{243}}\sqrt{41 + 40\cos(2t)}|3\rangle. \quad (61)$$

Calculating the time average,

$$\frac{1}{\pi} \int_0^\pi |\langle j|\tilde{\psi}(t)\rangle|^2 dt = \frac{101}{243}\delta_{j1} + \frac{101}{243}\delta_{j2} + \frac{41}{243}\delta_{j3}. \quad (62)$$

The numerical values of the CTQW and η-CTQW centrality rankings have been tabulated in Table I, alongside the classical PageRank ($\alpha = 0.85$) and eigenvector centrality rankings. Note that the two CTQW rankings strongly agree with the classical PageRank and eigenvector rank. Furthermore, the

TABLE I. Centrality ranking of the vertices of three-vertex graph (Fig. 1), using the classical PageRank method, the non-probability-conserving pseudo-Hermitian CTQW, and the probability-conserving pseudo-Hermitian CTQW (η-CTQW).

	Eigenvector	PageRank	CTQW	η-CTQW
1	0.5	0.475	0.416667	0.415638
2	0.5	0.475	0.416667	0.415638
3	0	0.05	0.166667	0.168724

numerical values of the two CTQW rankings only differ by a maximum of about 1.23%, indicating that the pseudo-Hermitian similarity transform preserves information regarding vertex centrality in this particular example. A general statistical analysis will be carried out in the subsequent section.

Let us now consider a four-vertex pseudo-Hermitian directed graph, as shown in Fig. 6. Note that this graph is composed of two sets of equivalent vertices: vertices 1 and 3 (in-degree $= 2$ and out-degree $= 1$), and vertices 2 and 4 (in-degree $= 1$ and out-degree $= 2$). Like the three-vertex graph analyzed previously, the CTQW probability can also be solved exactly, and thus the same method is applied to determine the vertex centrality.

The results of the CTQW and η-CTQW centrality test can be seen in Table II. In this case, both CTQW formulations and the eigenvector centrality ranked vertices 1 and 3 above vertices 2 and 4. Intuitively, this is perhaps expected, as vertices 1 and 3 have a greater in-degree and lower out-degree than vertices 2 and 4, resulting in walker probability accumulating on these two vertices. Interestingly, the classical PageRank measure does not distinguish between these two sets of vertices, as the limiting distribution of a (classical) random walk on this graph results in a unitary distribution. The agreement of the CTQW-based measures to the eigenvector centrality, as opposed to the PageRank, lends further credence to the suggestion that the CTQW measures centrality via a similar process to the eigenvector centrality.

As a final example, we briefly examined a pseudo-Hermitian interdependent network consisting of a four-vertex directed graph and a three-vertex directed graph, connected via complete interconnections (i.e., $B_0 = J$). The graph and various centrality rankings of the vertices are shown in Fig. 7;
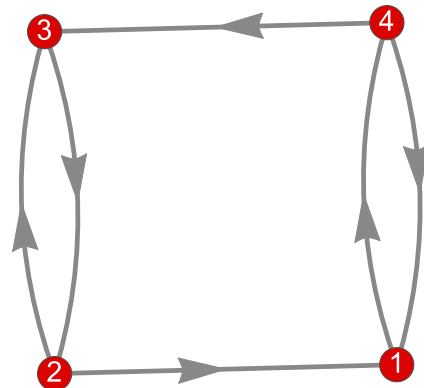

FIG. 6. Four-vertex directed graph.

TABLE II. Centrality ranking of the four vertices of Fig. 6, using the classical PageRank method, the non-probability-conserving pseudo-Hermitian CTQW, and the probability-conserving pseudo-Hermitian CTQW (η-CTQW).

	Eigenvector	PageRank	CTQW	η-CTQW
1	0.292893	0.25	0.386364	0.339192
2	0.207107	0.25	0.113636	0.160808
3	0.292893	0.25	0.386364	0.339192
4	0.207107	0.25	0.113636	0.160808

TABLE III. Vigna's τ rank correlation coefficient compared for various classical (PageRank and eigenvector) and quantum (nonunitary CTQW and pseudo-Hermitian η-CTQW) centrality measures applied to the seven-vertex interdependent network in Fig. 7.

	PageRank	Eigenvector	CTQW	η-CTQW
PageRank	1.0	0.912	0.937	0.896
Eigenvector	0.912	1.0	0.896	0.906
CTQW	0.937	0.896	1.0	0.761
η-CTQW	0.896	0.906	0.761	1.0

it can be seen that the pseudo-Hermitian η-CTQW centrality ranking strongly agrees with the classical PageRank and eigenvector results, with the only disagreement involving the rankings of vertices 3 and 6, as well as 1 and 4 (both display degeneracy in the classical measures), Fig. 7. Of note, the η-CTQW does a better job of ranking the vertices than the standard nonunitary CTQW in this case, perhaps indicating that the pseudo-Hermitian CTQW, itself a mapping
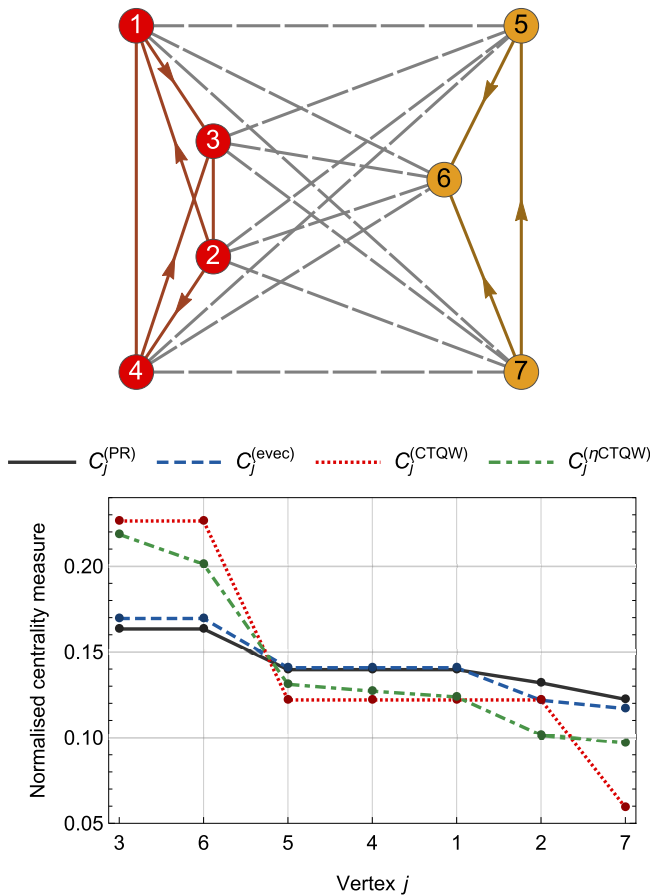

FIG. 7. Top: interdependent network, consisting of a directed four-vertex graph (red) connected to a directed three-vertex graph (yellow) via complete interconnections (gray, dashed line). Above: centrality ranking of the vertices, ordered from highest ranking to lowest ranking vertex. Measures used include the classical PageRank (black, solid line), the eigenvector centrality (blue, dashed line), the standard CTQW (red, dotted line), and the pseudo-Hermitian η-CTQW (green, dotted-dashed line).

of a directed graph to an undirected, yet weighted, complete graph, provides a better overall picture of the vertex ranks. In particular, the η-CTQW is the only ranking to break the top-ranked tie seen in the other measures, assigning slightly more importance to vertex 3 compared to vertex 6.

Another method of quantifying the correlation between the various centrality methods is to calculate their rank correlation coefficients. One such metric is Kendall's rank correlation coefficient, commonly referred to as Kendall's τ coefficient [63]. By counting the number of pairwise disagreements between two ranked lists of length N, and dividing by normalization factor $\binom{N}{2}$, Kendall's τ may take values $-1 \leqslant \tau \leqslant 1$, where $\tau = 1$ denotes perfect agreements between the ranked lists, $\tau = 0$ denotes no correlation, and $\tau = -1$ denotes perfect anticorrelation (i.e., one list is the reverse of the other). In the field of centrality analysis, Kendall's τ has become the definitive metric [64–67], by means of its ubiquity, efficient computability [68], and the fact that variants exist that take into account ties [69]. Despite this, Kendall's τ coefficient is not particularly suited towards comparing centrality measures. Measures with highly correlated top-ranked vertices may produce comparatively low τ values, as Kendall's τ equally weights all discordant pairs, regardless of where they appear in the ranking. Recently, weighted modifications have been proposed, specifically catered to comparing centrality measures, which use a hyperbolic weighting function to more heavily weight correlations of the top-ranked vertices. These include the AP (average precision) correlation [70] and Vigna's τ correlation coefficient [71]. As Vigna's τ further takes into account ties, we will apply Vigna's τ correlation coefficient to analyze the results of Fig. 7.

The results of this analysis can be seen in Table III. All compared centralities display very high correlation ($\tau \geqslant 0.8$), with the exception of the CTQW and η-CTQW, with a correlation value of $\tau = 0.761$ (still a significant result). This is most likely due to the degeneracy seen in the CTQW ranking, which is completely broken in the η-CTQW; these resulting ties slightly lower the τ value, even though they do not cause disagreeing rankings per se. Finally, note that the η-CTQW achieves its highest correlation value with the eigenvector centrality at $\tau = 0.906$, edging out correlation with the PageRank at $\tau = 0.896$.

In these three examples, we have seen that the pseudo-Hermitian CTQW preserves the vertex centrality information from the original directed graphs, resulting in a vertex rank identical (barring broken degeneracy) to the classical PageRank. While these relatively small examples allow us

to verify the results of the centrality ranking by intuitively and qualitatively examining the graph structures by eye, this analysis is not sufficient to ensure that the centrality ranking proposed here generalizes to other PT-symmetric graph structures. To do so, a statistical analysis featuring randomly generated directed graphs is required.

C. Random directed networks

To investigate the reliability of the pseudo-Hermitian CTQW on directed graphs, a statistical analysis will be undertaken using randomly generated directed networks. Here, we consider two classes of random networks: Erdős-Rényi networks and scale-free networks.

A random Erdős-Rényi graph, denoted $G(N,p)$, is comprised of N vertices with edges randomly distributed via a Bernoulli distribution with probability p. For such a network, the vertex degree distribution $P(k)$ (the fraction of vertices with degree k) is binomial in form,

$$P(k) = \binom{N-1}{k} p^k (1-p)^{N-k-1}, \tag{63}$$

resulting in most vertices with degree close to np, the mean number of connections [72,73]. In order to produce a PT-symmetric directed graph satisfying the Erdős-Rényi degree distribution, we take three approaches. First, we generate numerous directed Erdős-Rényi graphs (with parameters $N = 15$, $p = 0.3$) using the Python software package NETWORKX [74], and selecting from these 300 which satisfy pseudo-Hermiticity. An example is presented in Fig. 8, alongside a plot of the PageRank, nonunitary CTQW, and η-CTQW centrality measures for the pictured example. In this particular example, all three measures agree on the location of the top two ranked vertices, with slight discrepancies for the remaining vertices. Note that, from here onward, the classical eigenvector centrality is no longer included as a comparison, as we can no longer guarantee its performance; a majority of the graphs in this and subsequent ensembles contain acyclic and nonstrongly connected components that result in an eigenvector centrality value of zero.

Our second approach to generating pseudo-Hermitian directed Erdős-Rényi networks was motivated by computational constraints with using NETWORKX, and a desire to generate larger pseudo-Hermitian graphs in a slightly more systematic way. Here, we first create an undirected graph of N vertices with edges given by Bernoulli distribution with probability p. We then upper triangularize the resulting adjacency matrix, by setting everything below the diagonal to zero, in effect, imbuing direction on every edge in a systematic fashion. By restricting the adjacency matrix to be triangular, it is trivial to see that the Hamiltonian will also be triangular, with eigenvalues given by the diagonal elements of H, the set of vertex in-degree:

$$\lambda = \{\deg^-(v_i) | i = 1, \ldots, N\}, \tag{64}$$

where $\deg^-(v_i)$ is a function returning the in-degree of vertex v_i. As such, we ensure a real eigenspectrum, and simply restrict our random graph generator to output graphs with diagonalizable Hamiltonians in order to guarantee pseudo-Hermiticity. Note that, as the adjacency matrix is triangular,
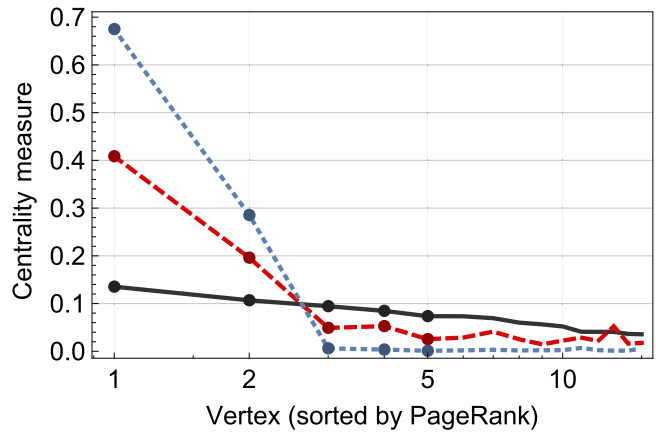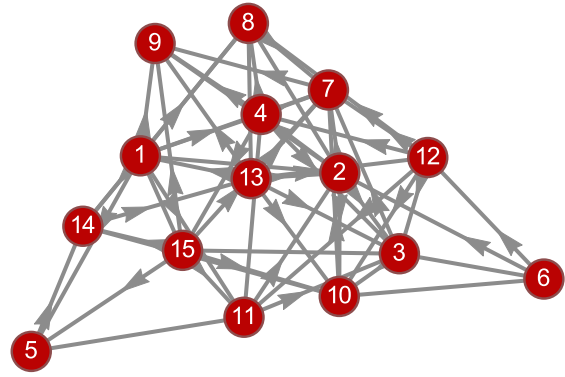

FIG. 8. Top: randomly generated pseudo-Hermitian Erdős-Rényi graph $G(15,0.3)$, with bidirectional edges allowed. Above: centrality ranking of the vertices, ordered from most central to least central as per the classical PageRank (black, solid line). This is compared to the nonunitary CTQW (blue, dotted line) and pseudo-Hermitian η-CTQW (red, dashed line).

all graphs in this ensemble are directed acyclic graphs, and thus the classical eigenvector centrality no longer produces useful results (it assigns all vertices a centrality measure of zero).

An example of a randomly generated pseudo-Hermitian directed Erdős-Rényi graph using this method is shown in Fig. 9, generated with parameters $N = 25$ and $p = 0.3$, alongside the results of the PageRank and η-CTQW centrality measures. It can be seen that the η-CTQW and the PageRank strongly agree on the relative vertex rankings, identically ranking the top four most central vertices, and satisfying the same general trend thereafter. This indicates that the η-CTQW continues to yield an admissible vertex centrality measure for larger, randomly generated graphs than in the previous section.

In the above two methods of pseudo-Hermitian Erdős-Rényi network generation, we are able to generate random graphs with bidirectional edges (allowing information to flow cyclically) and directed acyclic graphs, respectively. While only the former will permit use of the eigenvector centrality, the η-CTQW centrality algorithm may provide a usable centrality measure over both classes. To get a better understanding of how the η-CTQW centrality measure behaves over directed graph structures, we therefore introduce a third
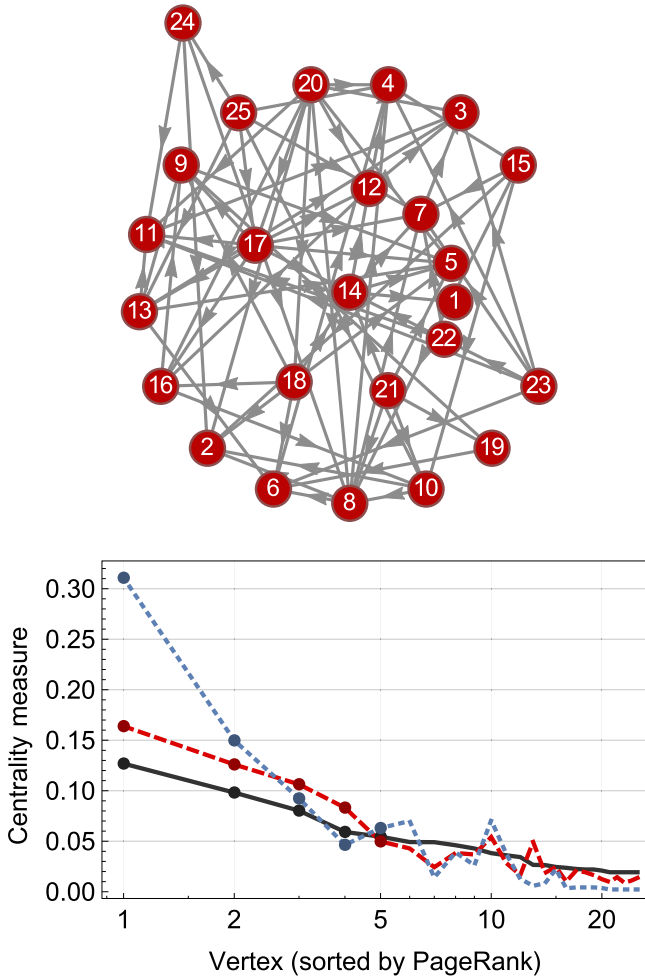
existing vertices with higher degrees (with probability of being connected to vertex i given by $p_i = k_i / \sum_j k_j$). This process continues until we have a graph containing the required number of vertices.

A fortunate side effect of the directed Barabási-Albert algorithm is that if we choose all m edges introduced with each additional vertex to be *inward*-pointing edges [resulting in $\deg^-(v_i) = m \ \forall \ i$], then the graph is necessarily lower triangular, leading to a Hamiltonian with real eigenspectrum as given by Eq. (64). Similarly, if we choose all m edges introduced with each vertex to be *outward*-pointing edges [resulting in $\deg^+(v_i) = m \ \forall \ i$], the Hamiltonian will be upper triangular and Eq. (64) continues to hold. Thus, like the Erdős-Rényi case described previously, to ensure pseudo-Hermiticity we simply ensure the resulting randomly generated scale-free Hamiltonian is diagonalizable. As before, the directed Barabási-Albert algorithm leads to the generation of directed acyclic graphs.

Figure 10 shows a pseudo-Hermitian directed graph constructed via the Barabási-Albert algorithm with parameters $N = 25$, $m = 4$, such that the in-degree vertex distribution is scale free. By examining the classical PageRank and η-CTQW centrality measures, we see that they provide identical rankings for all 20 vertices, correctly picking out and ordering the four "hubs" (marked in red) with larger in-degree. Meanwhile, in Fig. 11 we have a pseudo-Hermitian directed graph constructed via the Barabási-Albert algorithm with parameters $N = 100$, $m = 3$, such that the *out-degree* is scale free, and constant in-degree of 3. Again, the PageRank and η-CTQW display a high correlation, with the ranking of the top four most central vertices identical. However, in this case a subtlety must be addressed: the PageRank algorithm is known to correlate with in-degree [79,80], as is the η-CTQW scheme by construction of the Hamiltonian in Eq. (2). Hence, rather than assigning higher measures to vertices that are out-degree hubs, both algorithms are preferentially selecting top-ranked vertices based on in-degree distribution. These correspond to the vertices at which the probability flow of a random walk is likely to accumulate after significant time.

FIG. 9. Top: randomly generated directed pseudo-Hermitian Erdős-Rényi graph $G(25,0.3)$, where every edge is directed. Above: centrality ranking of the vertices, ordered from most central to least central as per the classical PageRank (black, solid line). This is compared to the nonunitary CTQW (blue, dotted line) and pseudo-Hermitian η-CTQW (red, dashed line).

method of pseudo-Hermitian Erdős-Rényi network generation, an intermediary between the two previously discussed classes. Here, we generate pseudo-Hermitian Erdős-Rényi networks as per our second (directed acyclic) approach, before introducing one bidirectional edge to the structure. Due to this addition, the overall graph is no longer directed acyclic, however, all but one vertex form a directed acyclic subgraph.

Scale-free networks, compared to Erdős-Rényi networks, exhibit a power law degree distribution of the form $P(k) \sim k^{-\gamma}$, due to a few very strongly connected vertices or "hubs," with a majority of vertices in the structure having significantly lower degree [75,76]. As such, this makes them well suited to modeling a wide array of physical systems and networks with similar characteristics, for example, power grids, the World Wide Web, social networks, and biochemical molecules [77,78]. To generate random pseudo-Hermitian scale-free graphs, we make use of the directed Barabási-Albert algorithm: at each time step, a vertex with m directed edges is introduced to the system, and preferentially attached to

D. Statistical analysis

So far, we have considered particular Erdős-Rényi and scale-free randomly generated graphs; to explore how the pseudo-Hermitian CTQW centrality scheme behaves in general, it is pertinent to undertake a statistical analysis of an ensemble of random graphs. Ensembles of 300 random Erdős-Rényi ($N = 25$, $p = 0.3$, random bidirectional edges permitted), 100 random Erdős-Rényi ($N = 25$, $p = 0.3$, one bidirectional edge permitted), 100 random Erdős-Rényi ($N = 25$, $p = 0.3$, directed acyclic), 100 random in-degree scale free ($N = 20$, $m = 3$), and 100 random out-degree scale free ($N = 40$, $m = 3$) were generated, and the PageRank, nonunitary CTQW, and η-CTQW vertex ranking determined for each graph. The mean and standard deviations of these centralities are plotted in Fig. 12 (for Erdős-Rényi ensembles) and Fig. 13 (for scale-free ensembles), with the η-CTQW compared to both the nonunitary CTQW and classical PageRank. Furthermore, Vigna's τ rank correlation coefficient has been averaged across the ensemble, and is displayed on each plot.
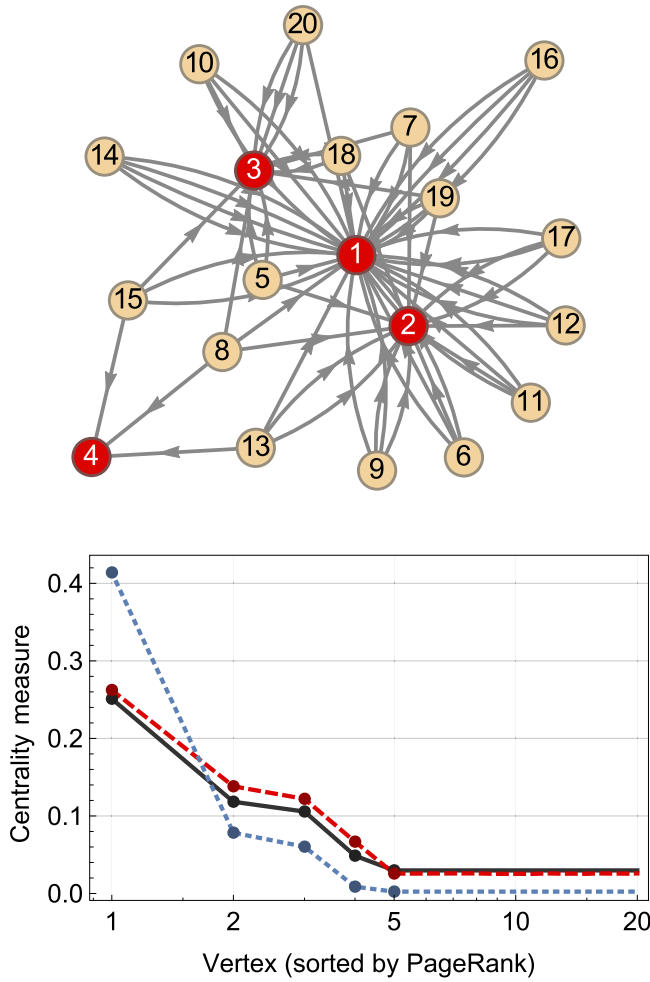
FIG. 10. Top: randomly generated 20-vertex pseudo-Hermitian graph, with scale-free in-degree distribution where $m = 4$. The more highly connected "hubs" (vertices with higher in-degree) are labeled in red. Above: centrality ranking of the vertices, ordered from most central to least central as per the classical PageRank (black, solid line). This is compared to the nonunitary CTQW (blue, dotted line) and the pseudo-Hermitian η-CTQW (red, dashed line).

Studying the results of Figs. 12 and 13, we may draw several conclusions. First, the η-CTQW continues to reflect the directed structure of the network, agreeing with the nonunitary CTQW across all ensembles on the top five ranked vertices. This agreement is similarly reflected in Vigna's tau correlation coefficient, with $\tau \geqslant \sim 0.6$ for every ensemble, with lower values perhaps due to small discrepancies for lower ranked vertices.

Still, this statistical analysis has its drawbacks. The shaded areas, representing one standard deviation from the mean centrality values, indicate general ranking agreement across an ensemble *only* when narrow enough and with a steep enough gradient such that each consecutive point, when moved upward or downward by one standard deviation, does not cause a swap in ranking [e.g., Fig. 13(a)]. Further, the converse is not true: a large standard deviation does not imply a lack of agreement in ranking. In fact, two centrality measures could produce the exact same ranking across an entire ensemble, yet one measure might simply have a greater variance in the values it assigns
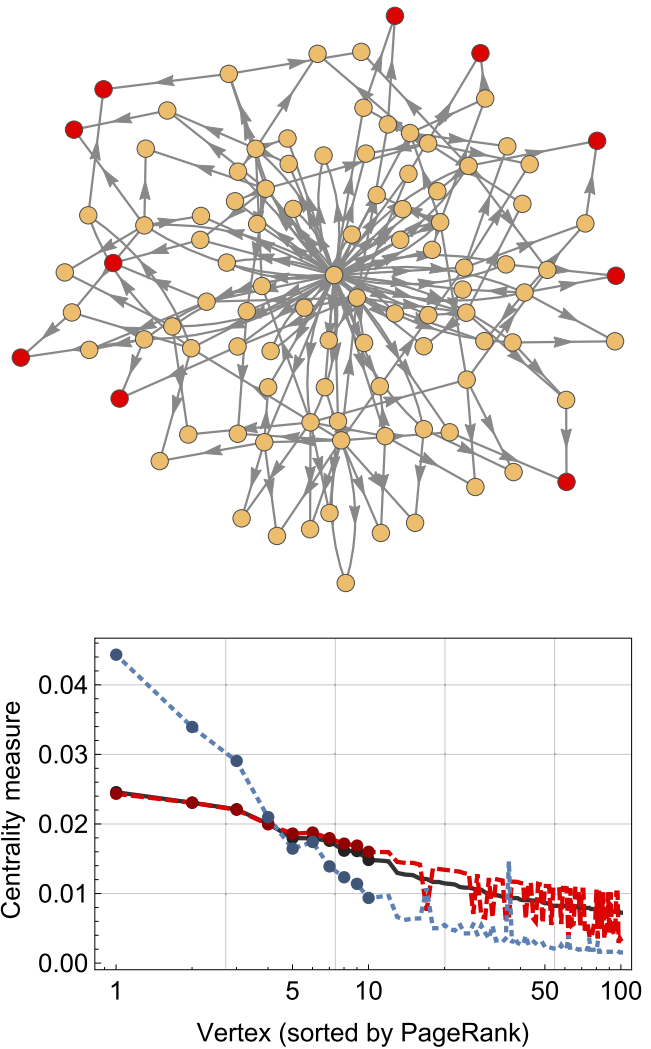

FIG. 11. Top: randomly generated 100-vertex pseudo-Hermitian graph, with scale-free out-degree distribution where $m = 3$. The top 10 vertices where network flow is likely to accumulate are labeled in red. Above: centrality ranking of the vertices, ordered from most central to least central as per the classical PageRank (black, solid line). This is compared to the nonunitary CTQW (blue, dotted line) and the pseudo-Hermitian η-CTQW (red, dashed line).

to the vertices. Similarly, Vigna's τ correlation coefficient, while a better indicator of overall rank agreement, continues to suffer from the fact that small discrepancies in ranking of lower-ranked vertices negatively affect the coefficient value. Thus, while these approaches might be useful in determining correlation between various centrality measures, they distract from the main question: How frequently do two centrality measures agree on the k topmost ranked vertices?

In order to answer this quantitatively, we employ the Jaccard measure of set similarity [81]. This provides an indicator of how well each centrality measure is able to determine the identity of the top k highest centrality individuals. First, for each graph, unordered sets containing the n most central vertices according to each measure were compared, the fraction of matching vertices providing a quantitative value
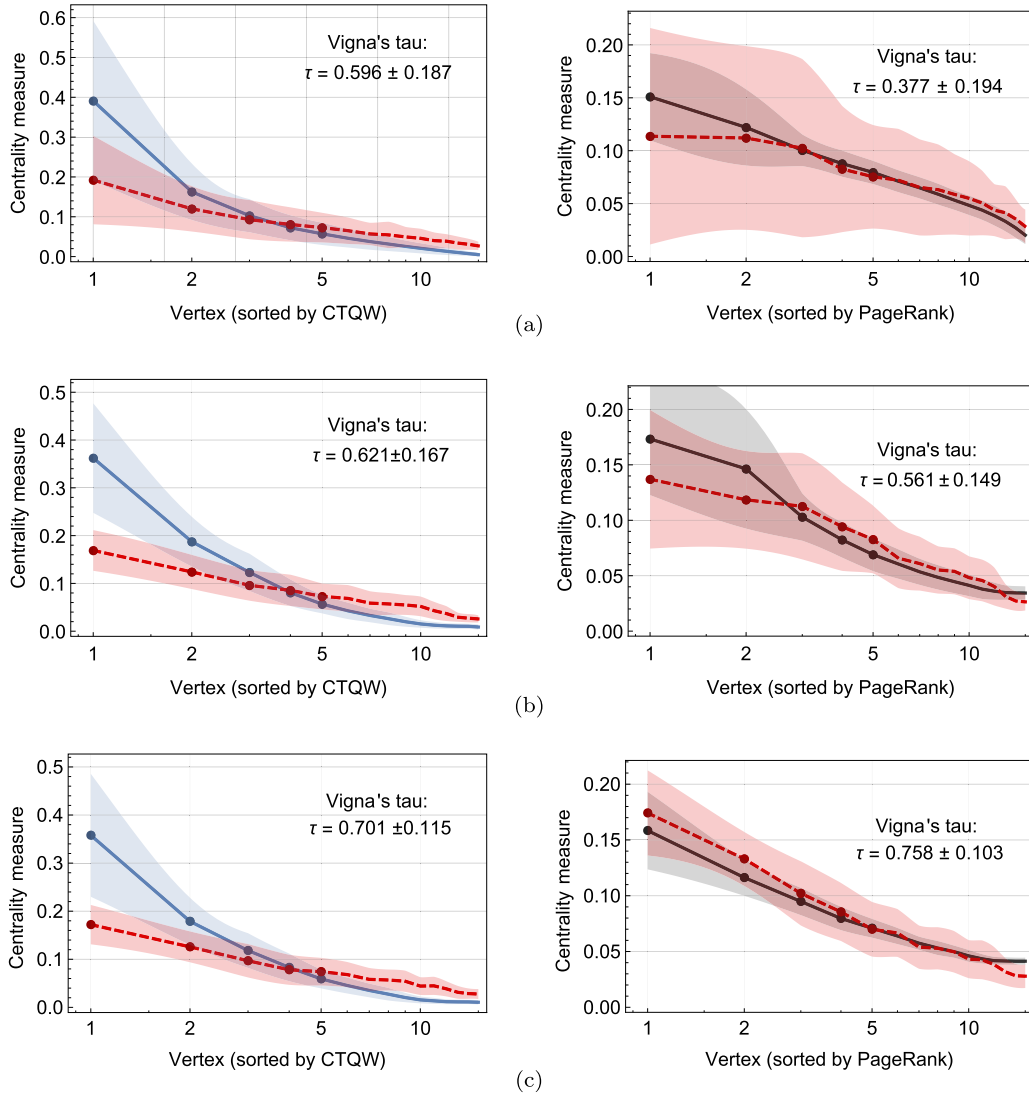
FIG. 12. Centrality measure values for the pseudo-Hermitian η-CTQW (red, dashed line), compared against the non-unitary CTQW ranking (blue), and PageRank ranking (black), averaged over an ensemble of (a) 300 Erdős-Rényi graphs with random bidirectional edges, (b) 100 Erdős-Rényi graphs with one bidirectional edge, (c) 100 Erdős-Rényi directed acyclic graphs.

for the agreement between the two measures. Finally, these were averaged over the entire ensemble, providing a general measure of the agreement between the PageRank and the η-CTQW, with uncertainty approximated by calculating the Agresti-Coull 95% confidence interval [82]. The results of the statistical analysis are presented in Fig. 14. When considering just the most central vertex, the PageRank and η-CTQW are in excellent agreement in the case of the directed acyclic Erdős-Rényi and scale-free ensembles, ranging from 95% to 100% agreement. As the number of vertices compared increases, there is a small decrease in the Jaccard set similarity, with all three ensembles of random graphs exhibiting agreement factors in the range of 90% for the top two and three most central vertices. By the time we consider five vertices, scale-free networks retain an excellent agreement of 100% and 92%, while the directed acyclic Erdős-Rényi ensemble exhibits a reasonably good agreement factor of 78%. These trends can be partially explained by considering the behavior of the degree distributions:

(i) Erdős-Rényi networks, with a majority of vertices having degree close to the mean, generally result in the highest ranked vertices having similar centrality measures. As such, beyond the top three, small variations in the PageRank and η-CTQW vertex ordering appear, leading to discrepancies.

(ii) In-degree scale-free networks, with a small number of highly connected vertices, should easily distinguish these vertices (the hubs) as most central to the network. Beyond the hubs, the power law characteristic results in the majority of remaining vertices having similar degree, leading to small variations in vertex ordering, and thus the discrepancies observed between the PageRank and η-CTQW as more vertices are compared.

However, comparing the η-CTQW and PageRank for the nondirected acyclic Erdős-Rényi ensembles (those with bidirectionality of edges permitted), we see a significant reduction in the agreement of the top five vertices. For instance, in Fig. 14, it can be seen that topmost vertex Jaccard set similarity between the PageRank and η-CTQW
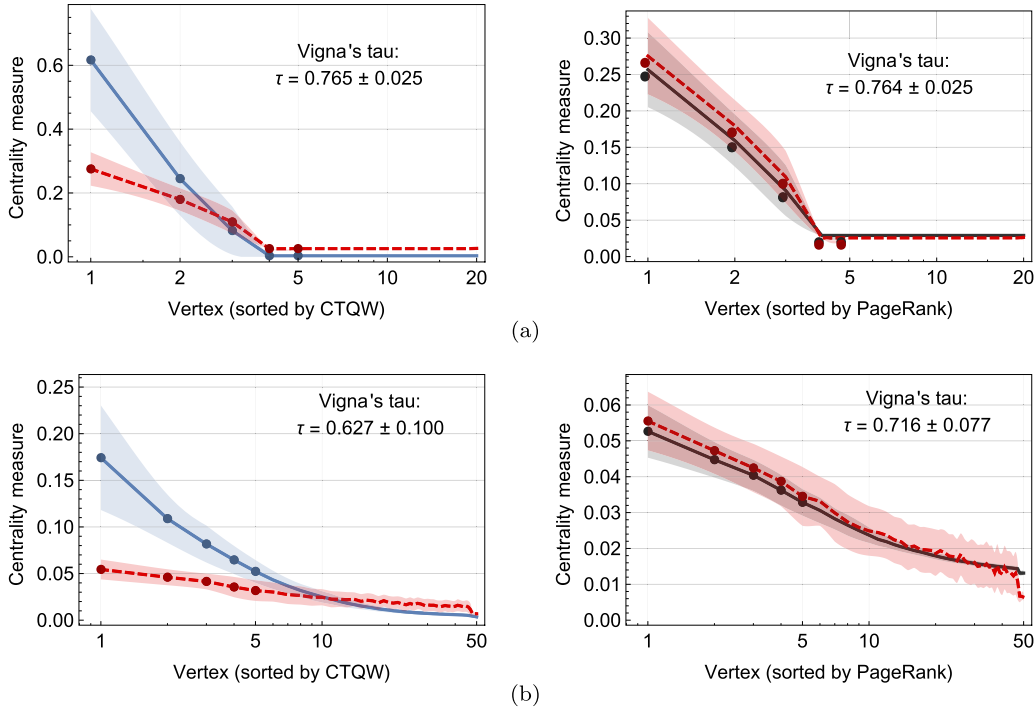
FIG. 13. Centrality measure values for the pseudo-Hermitian η-CTQW (red, dashed line), compared against the nonunitary CTQW ranking (blue), and PageRank ranking (black), averaged over an ensemble of (a) 100 directed in-degree scale-free graphs, and (b) 100 directed out-degree scale-free graphs. The shaded areas represent the region within one standard deviation of the mean.

on the ensemble with one permitted bidirectional edge is 43%; this drops to 13% when random bidirectional
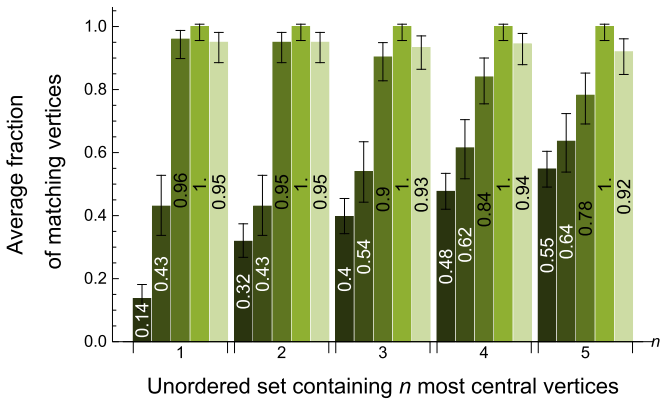

FIG. 14. Chart showing the Jaccard set similarity between the classical PageRank algorithm and the η-CTQW centrality scheme for an ensemble of 300 directed Erdős-Rényi graphs with bidirectional edges permitted, 100 directed Erdős-Rényi graphs with undirected edges, 100 directed in-degree scale-free graphs, and 100 directed out-degree scale-free graphs. Each bar represents the unordered set containing the n most central vertices as determined by the PageRank and η-CTQW scheme, while the vertical axis gives the average fraction of matching vertices between these two sets. The error bars indicate the Agresti-Coull 95% confidence interval.

edges are permitted. This could be due to a multitude of factors:

(1) The PageRank might provide a significantly different rank to other classical measures, which the η-CTQW is more inclined to agree with; this difference may be magnified on nondirected acyclic graphs.

(2) Localization of the η-CTQW may be occurring, due to either classical effects [59,62] or quantum effects (Anderson localization).

Interestingly, the η-CTQW centrality measure appears to allows us to apply an eigenvectorlike quantum centrality algorithm that agrees readily with the classical PageRank on directed acyclic graphs, on which the eigenvector centrality provides inconclusive results, while failing to agree with PageRank on nondirected acyclic graphs.

Ultimately, whatever the reason, further investigation is required to determine the likely cause of the discrepancy. Note that this is not a negative result per se, depending on the model represented by the graph structure, the η-CTQW could be providing a better result of marking influential and central nodes. However, this analysis is beyond the scope of this paper, and is reserved for future research. Nevertheless, the results presented here show that the η-CTQW provides centrality rankings for several classes of randomly generated graphs that are consistent with the classical PageRank algorithm.

VI. CONCLUSION

In this paper, we have introduced and expanded a framework for continuous-time quantum walks on directed graphs, by utilizing PT symmetry. In the case of interdependent networks of directed graphs, a sufficient condition for ensuring

PT symmetry was detailed, and the directed walk formalism was shown to be equivalent to simulating a continuous-time quantum walker on an undirected, weighted, complete graph with self-loops. This may potentially lead to easily implementable experimental directed continuous-time quantum walks.

Finally, we have introduced a quantum scheme for centrality testing on directed graphs, by utilizing PT-symmetric continuous-time quantum walks; unlike other directed quantum-walk-based centrality measures, our method does not require expanding the Hilbert space to ensure unitary behavior. A statistical analysis was performed, confirming the CTQW centrality measure proposed here is consistent with classical centrality measures for various classes of randomly generated directed acyclic graphs.

Preliminary results on four-vertex pseudo-Hermitian directed graphs have shown that the CTQW centrality ranking is able to distinguish nonequivalent sets of vertices that the classical PageRank cannot. This is likely due to the CTQW providing an eigenvectorlike centrality measure in the quantum regime; calculating the rank correlation coefficients supports this interpretation. However, further work is required to fully understand the distinguishing power of the pseudo-Hermitian CTQW centrality measure.

Quantum walks remain an important physical tool, linking the fields of information theory, quantum computation, and complex quantum dynamical modeling. Following on from this work, we aim to utilize the PT-symmetric CTQW framework to model and simulate behavior in physical biochemical systems, such as electron or exciton transport. Future work will also involve exploring methods of implementing the PT-symmetric CTQW centrality scheme on physical systems.

[1] Y. Aharonov, L. Davidovich, and N. Zagury, Phys. Rev. A **48**, 1687 (1993).

[2] Q.-h. Wang, Philos. Trans. R. Soc. London, Ser. A **371**, 20120045 (2013).

[3] S. D. Berry and J. B. Wang, Phys. Rev. A **82**, 042333 (2010).

[4] S. D. Berry and J. B. Wang, Phys. Rev. A **83**, 042317 (2011).

[5] A. M. Childs and J. Goldstone, Phys. Rev. A **70**, 022314 (2004).

[6] B. L. Douglas and J. B. Wang, J. Phys. A: Math. Theor. **41**, 075303 (2008).

[7] A. M. Childs, R. Cleve, E. Deotto, E. Farhi, S. Gutmann, and D. A. Spielman, in *Proceedings of the Thirty-fifth Annual ACM Symposium on Theory of Computing, STOC '03* (ACM, New York, 2003), pp. 59–68.

[8] K. Rudinger, J. K. Gamble, E. Bach, M. Friesen, R. Joynt, and S. N. Coppersmith, J. Comput. Theor. Nanosci. **10**, 1653 (2013).

[9] A. Mahasinghe, J. A. Izaac, J. B. Wang, and J. K. Wijerathna, J. Phys. A: Math. Theor. **48**, 265301 (2015).

[10] G. D. Paparo, M. Müller, F. Comellas, and M. A. Martin-Delgado, Sci. Rep. **3**, 02773 (2013).

[11] M. Sarovar, A. Ishizaki, G. R. Fleming, and K. B. Whaley, Nat. Phys. **6**, 462 (2010).

[12] G. S. Engel, T. R. Calhoun, E. L. Read, T. Ahn, T. Mančal, Y. Cheng, R. E. Blankenship, and G. R. Fleming, Nature (London) **446**, 782 (2007).

[13] M. Mohseni, P. Rebentrost, S. Lloyd, and A. Aspuru-Guzik, J. Chem. Phys. **129**, 174106 (2008).

[14] P. Rebentrost, M. Mohseni, I. Kassal, S. Lloyd, and A. Aspuru-Guzik, New J. Phys. **11**, 033003 (2009).

[15] A. M. Childs, Phys. Rev. Lett. **102**, 180501 (2009).

[16] A. M. Childs, D. Gosset, and Z. Webb, Science **339**, 791 (2013).

[17] T. Loke, J. W. Tang, J. Rodriguez, M. Small, and J. B. Wang, Quantum Inf. Proc. **16**, 25 (2017).

[18] I. Sinayskiy and F. Petruccione, J. Phys.: Conf. Ser. **442**, 012003 (2013).

[19] C. M. Bender and S. Boettcher, Phys. Rev. Lett. **80**, 5243 (1998).

[20] A. Mostafazadeh, J. Math. Phys. **43**, 205 (2002).

[21] A. Mostafazadeh, J. Math. Phys. **43**, 3944 (2002).

[22] P. D. Mannheim, Philos. Trans. R. Soc. London, Ser. A **371**, 20120060 (2013).

[23] J. Li, Y. Miao, and Z. Xue, PLoS ONE **9**, e97107 (2014).

[24] B. Basu-Mallick and A. Kundu, Phys. Rev. B **62**, 9927 (2000).

[25] C. M. Bender, Czech. J. Phys. **54**, 13 (2004).

[26] C. M. Bender, H. F. Jones, and R. J. Rivers, Phys. Lett. B **625**, 333 (2005).

[27] X. Luo, J. Huang, H. Zhong, X. Qin, Q. Xie, Y. S. Kivshar, and C. Lee, Phys. Rev. Lett. **110**, 243902 (2013).

[28] B. Peng, C. K. Özdemir, F. Lei, F. Monifi, M. Gianfreda, G. L. Long, S. Fan, F. Nori, C. M. Bender, and L. Yang, Nat. Phys. **10**, 394 (2014).

[29] A. Regensburger, C. Bersch, M. Miri, G. Onishchukov, D. N. Christodoulides, and U. Peschel, Nature (London) **488**, 167 (2012).

[30] C. E. Rüter, K. G. Makris, R. El-Ganainy, D. N. Christodoulides, M. Segev, and D. Kip, Nat. Phys. **6**, 192 (2010).

[31] F. J. Dyson, Phys. Rev. **102**, 1217 (1956).

[32] F. H. M. Faisal and J. V. Moloney, J. Phys. B: At. Mol. Phys. **14**, 3603 (1981).

[33] K. Jones-Smith, Philos. Trans. R. Soc. London, Ser. A **371**, 20120056 (2013).

[34] K. Mochizuki, D. Kim, and H. Obuse, Phys. Rev. A **93**, 062116 (2016).

[35] S. Salimi and A. Sorouri, J. Phys. A: Math. Theor. **43**, 275304 (2010).

[36] J. A. Izaac, X. Zhan, Z. Bian, K. Wang, J. Li, J. B. Wang, and P. Xue, Phys. Rev. A **95**, 032318 (2017).

[37] S. Brin and L. Page, Comput. Networks ISDN Syst. **30**, 107 (1998).

[38] F. M. Fernández, R. Guardiola, J. Ros, and M. Znojil, J. Phys. A: Math. Gen. **32**, 3105 (1999).

[39] S. Weigert, J. Opt. B: Quantum Semiclassical Opt. **5**, S416 (2003).

[40] C. F. d. M. Faria and A. Fring, J. Phys. A: Math. Gen. **39**, 9269 (2006).

[41] A. Mostafazadeh, J. Math. Phys. **43**, 2814 (2002).

[42] L. Solombrino, J. Math. Phys. **43**, 5439 (2002).

[43] G. Scolarici and L. Solombrino, J. Math. Phys. **44**, 4450 (2003).

[44] C. M. Bender and P. D. Mannheim, Phys. Lett. A **374**, 1616 (2010).

[45] M. Anthony and M. Harvey, *Linear Algebra: Concepts and Methods* (Cambridge University Press, Cambridge, 2012).

[46] J. Gao, S. V. Buldyrev, H. E. Stanley, and S. Havlin, Nat. Phys. **8**, 40 (2012).

[47] V. Rosato, L. Issacharoff, F. Tiriticco, S. Meloni, S. D. Porcellinis, and R. Setola, Int. J. Critical Infrastruct. **4**, 63 (2008).

[48] C. Nehaniv, P. Dini, P. Van Mieghem, and P. Van Mieghem, Construction of Interdependent Networks and Efficiency Improvements in their Stability Calculation, Technical Report Technical No. FP7-288021, Information and Communication Technologies, 2014 (unpublished).

[49] D. Knoke and R. S. Burt, Appl. Network Anal., 195 (1983).

[50] D. J. Brass, Admin. Sci. Quarterly **29**, 518 (1984).

[51] H. Ibarra and S. B. Andrews, Admin. Sci. Quarterly **38**, 277 (1993).

[52] H. Ibarra, Acad. Management J. **36**, 471 (1993).

[53] D. S. Sade, Social Networks(Special Issue on Non-Human Primate Networks), **11**, 273 (1989).

[54] G. Amitai, A. Shemesh, E. Sitbon, M. Shklar, D. Netanely, I. Venger, and S. Pietrokovski, J. Mol. Biol. **344**, 1135 (2004).

[55] G. Lawyer, Sci. Rep. **5**, 8665 (2015).

[56] J. Liu, Z. Ren, and Q. Guo, Phys. A (Amsterdam) **392**, 4154 (2013).

[57] S. P. Borgatti, Social Networks **27**, 55 (2005).

[58] S. P. Borgatti and M. G. Everett, Social Networks **28**, 466 (2006).

[59] R. Pastor-Satorras and C. Castellano, Sci. Rep. **6**, 18847 (2016).

[60] P. Bonacich, Am. J. Sociol. **92**, 1170 (1987).

[61] N. Perra and S. Fortunato, Phys. Rev. E **78**, 036107 (2008).

[62] T. Martin, X. Zhang, and M. E. J. Newman, Phys. Rev. E **90**, 052808 (2014).

[63] M. G. Kendall, Biometrika **30**, 81 (1938).

[64] H. Kim and R. Anderson, Phys. Rev. E **85**, 026107 (2012).

[65] D. Chen, L. Lü, M. Shang, Y. Zhang, and T. Zhou, Phys. A (Amsterdam) **391**, 1777 (2012).

[66] A. Lulli, L. Ricci, E. Carlini, and P. Dazzi, in *2015 IEEE 9th International Conference on Self-Adaptive and Self-Organizing Systems* (IEEE, Piscataway, NJ, 2015), pp. 71–80.

[67] Y. Du, C. Gao, X. Chen, Y. Hu, R. Sadiq, and Y. Deng, Chaos **25**, 033112 (2015).

[68] W. R. Knight, J. Am. Stat. Assoc. **61**, 436 (1966).

[69] M. G. Kendall, Biometrika **33**, 239 (1945).

[70] E. Yilmaz, J. A. Aslam, and S. Robertson, in *Proceedings of the 31st Annual International ACM SIGIR Conference on Research and Development in Information Retrieval, SIGIR '08* (ACM, New York, 2008), pp. 587–594.

[71] S. Vigna, in *Proceedings of the 24th International Conference on World Wide Web, WWW '15* (International World Wide Web Conferences Steering Committee, Republic and Canton of Geneva, Switzerland, 2015), pp. 1166–1176.

[72] P. Erdős and A. Rényi, Publicationes Mathematicae (Debrecen) **6**, 290 (1959).

[73] P. Erdős and A. Rényi, in *Publication of the Mathematical Institute of the Hungarian Academy of Sciences* (Hungarian Academy of Sciences, Budapest, 1960), pp. 17–61.

[74] A. A. Hagberg, D. A. Schult, and P. J. Swart, in *Proceedings of the 7th Python in Science Conference*, edited by G. Varoquaux, T. Vaught, and J. Millman (Pasadena, CA, 2008), pp. 11–15, http://conference.scipy.org/proceedings/scipy2008/paper_2/.

[75] A. Barabási and R. Albert, Science **286**, 509 (1999).

[76] A. Barabási, R. Albert, and H. Jeong, Phys. A (Amsterdam) **281**, 69 (2000).

[77] R. Albert and A. Barabási, Rev. Mod. Phys. **74**, 47 (2002).

[78] C. Song, S. Havlin, and H. A. Makse, Nature (London) **433**, 392 (2005).

[79] N. Litvak, W. R. W. Scheinhardt, and Y. Volkovich, Internet Math. **4**, 175 (2007)

[80] S. Fortunato, M. Boguñá, A. Flammini, and F. Menczer, in *Algorithms and Models for the Web-Graph*, Vol. 4936, edited by W. Aiello, A. Broder, J. Janssen, and E. Milios (Springer, Berlin, 2008), pp. 59–71.

[81] A. S. Maiya and T. Y. Berger-Wolf, *Advances in Knowledge Discovery and Data Mining* (Springer, Berlin, 2010), pp. 91–98.

[82] A. Agresti and B. A. Coull, Am. Stat. **52**, 119 (1998).